Supporting Information

Porous platinum nanotubes modified with dendrimers as nanocarriers and electrocatalysts for sensitive electrochemical aptasensor based on enzymatic signal amplification

Wenju Xu*, Yongmei Wu, Huayu Yi, Lijuan Bai, Yaqin Chai, Ruo Yuan*

Chongqing Key Laboratory of Analytical Chemistry, Education Ministry Key Laboratory on Luminescence and Real-Time Analysis, School of Chemistry and Chemical Engineering, Southwest University, Chongqing 400715, China

EXPERIMENTAL SECTION

Reagents and Materials:

Thrombin (TB), hexanethiol (96%, HT), horseradish peroxidase (HRP), 3-(mercaptopropyl)trimethoxysilane (MPTS), toluidine blue (Tb), gold chloride ($HAuCl_4$), chloro platinic acid (H_2PtCl_6), hexadecyltrimethylammonium bromide (CTAB, 99%), sodium dodecyl sulfate (SDS, 99%), bovine serum albumin (BSA), carcinoembryonic antigen (CEA), hemoglobin (Hb) and L-cysteine (L-cys) were obtained from Sigma-Aldrich Chemical Co. (St. Louis, MO, USA). Amine-terminated polyamidoamine (PAMAM, G 5.0) dendrimer was supplied by Aldrich (St. Louis, MO, USA). Tellurium dioxide powder (TeO_2, 99.9%) was purchased from Shanghai Zhi Xin Chemical Co. (China). Glutaraldehyde (GA) was obtained from Beijing Chemical Reagent Co. (Beijing, China). Thrombin binding aptamer (TBA): 5'-NH_2-$(CH_2)_6$-GGT TGG TGT GGT TGG-3' was synthesized from TaKaRa (Dalian, China).

Tris-hydroxymethylaminomethane hydrochloride (Tris-HCl) was purchased from Roche (Switzerland). 20 mM Tris-HCl buffer (pH 7.4) containing 140 mM NaCl, 5 mM KCl, 1 mM $CaCl_2$ and 1 mM $MgCl_2$ served as binding buffer. 0.1 M phosphate buffered solution (PBS, pH 7.0) containing 10 mM Na_2HPO_4 and 10 mM KH_2PO_4 was used as working buffer. All other chemicals used were of reagent grade and directly used as received. Double distilled water was used through this work.

Apparatus:

Differential pulse voltammetry (DPV), cyclic voltammetry (CV) and electrochemical impedance spectroscopy (EIS) measurements were carried out with a CHI 660D electrochemical workstation (Shanghai Chenhua Instrument, China). A three-electrode system, including the modified glassy carbon electrode (GCE, Φ = 4 mm) as working electrode, a platinum wire as the counter electrode and a saturated calomel electrode (SCE) as the reference electrode, was employed for the above electrochemical measurement. pH measurement was carried out with a pH meter (MP 230, Mettler-Toledo, Switzerland). Transmission electron microscope (TEM) images were recorded on a JEOL, JEM-2100 transmission electron microscope. The scanning electron micrographs were taken with scanning electron microscope (SEM, S-4800, Hitachi). Ultraviolet-visible (UV-vis) absorption spectra were recorded with an UV-vis 2450 spectrophotometer (Tokyo, Japan).

Preparation of porous platinum nanotubes (PtNTs):

Porous PtNTs were synthesized according to the procedure proposed by Cai and coworker.[1] According to the literature,[2] tellurium nanowires (TeNWs) were firstly

prepared by slowly adding hydrazine monohydrate (5 mL) to the breaker containing tellurium dioxide (0.032 g) at room temperature, followed by constant magnetic stirring the resulting solution for 60 min to the point at which it turned from colorless to blue, which indicated the successful formation of TeNWs.[2] In order to terminate the reaction and stabilize the resultant, the blue solution was diluted 10-fold with SDS (10 mM), centrifuged and washed for several times, and TeNWs were collected for further use. Subsequently, approximately 0.01 mmol of the as- prepared TeNWs was dispersed in CTAB (10 mL, 1 mM) under constant magnetic stirring for 15 min. H_2PtCl_6 (~0.002 mmol) was adjusted to pH 7.0 using NaOH (0.1 M) and added into the above TeNWs mixture. After stirring for 50 min, changing of the color of resulting solution from blue to grey black showed the formation of Te@Pt core-shell nanostructure.[1] Another centrifugation and washing were carried out to abandon the surplus matrices, including CTAB. The obtained intermediate product (Te@Pt) was re-suspended in water (0.5 mL) and kept for about 3 h at room temperature. Finally, PtNTs with high porosity were obtained by further centrifugation and washing, and re-dispersed in PBS (pH 7.0) for further use.

Preparation of PtNTs-PAMAM-Tb-TBA-BSA bioconjugate (secondary aptamer):

Initially, amine-terminated PAMAM (0.07 mM) was added into the as-prepared porous PtNTs (1 mL) and then stirred for 10 h till PtNTs-PAMAM nanocomposites were obtained via the conjugate between PtNTs and amine groups of PAMAM. Excess PAMAM was removed by centrifugation and washing. Then, Tb (500 μL, 3 mM) and TBA (100 μL, 2.0 μM) were added into the above PtNTs-PAMAM solution and stirred

overnight at 4 ºC. Tb with -NH_2 group and amido-terminated TBA were attached onto PtNTs-PAMAM nanocomposites along with GA as the linking agent by the amine-aldehyde reaction. 100 μL BSA (w/w, 1 %) was then added into the solution and incubated for 40 min to block the remaining active sites on Tb and TBA labeled PtNTs-PAMAM nanocomposites. Finally, PtNTs-PAMAM-Tb-TBA-BSA bioconjugate was obtained by further centrifugation and re-dispersed in 1 mL PBS (pH 7.0) for further use. All the above experiments were performed at 4 ºC.

Preparation of MPTS sol-HRP biocomposite:

MPTS sol-HRP biocomposite was prepared according to the literature[3] with a little modification. The synthesis procedure was divided into two portions: Firstly, MPTS sol was obtained by taking MPTS (24 μL) and HCl (0.1 M, 10 μL) into 2 mL water, and the resulting mixture was vigorously stirred for 30 min. Secondly, the as-formed MPTS-sol (500 μL) was mixed with HRP (500 μL), followed by gently stirring for 2-3 min. Thus, HRP enzyme could be embedded in the three-dimensional network of MPTS, resulting in the formation of MPTS sol-HRP biocomposite. The prepared biocomposite was stored at 4 ºC for further use.

Fabrication of the proposed electrochemical aptasensor:

The stepwise assembly of modified electrode was illustrated in Scheme 1. A bare GCE was polished to mirror-like by using 0.3 and 0.05 μm Al_2O_3 powder successively, followed by sonication in ethanol and water. Then gold nanoparticles (AuNPs) were electrodeposited on the cleaned and dried GCE surface in 2 mL $HAuCl_4$ (1 %) aqueous solution under the potential –0.2 V for 30 s. Next, 5 μL of MPTS sol-HRP

biocomposite was coated on the resulting GCE and dried at 4 ºC, leading to assembling of MPTS sol-HRP on the modified electrode via Au-S affinity. In order to capture TBA, AuNPs was further electrodeposited onto the modified electrode in a similar way. Subsequently, 20 μL of TBA (2 μM) in Tris-HCl buffer (pH 7.4) was incubated onto the modified electrode for 16 h at 4 ºC to obtain TBA/AuNPs/MPTS sol-HRP/ AuNPs/GCE. After rinsing with double distilled water, the modified electrode was dipped into HT (20 μL, 1.0 mM) solution for 40 min to block possible residual sites on AuNPs layer against nonspecific adsorption. Ultimately, the HT/TBA/AuNPs/MPTS sol-HRP/AuNPs modified GCE was obtained and stored at 4 ºC when not in use.

Experimental measurements:

20 μL TB with various concentrations in Tris-HCl buffer (pH 7.4) was placed on the HT/TBA/AuNPs/MPTS sol-HRP/AuNPs modified electrode for 40 min. Then, 20 μL secondary aptamer (PtNTs-PAMAM-Tb-TBA-BSA bioconjugate) was incubated onto the resulting modified electrode for 40 min, and its DPV response was recorded in 2 mL PBS (0.1 M, pH 7.0) with a potential range of 0.1 V to –0.6 V, modulation amplitude of 0.05 V, pulse width of 0.05 s and sample width of 0.0167 s. Additionally, CV and EIS investigation were performed in 2 mL PBS (0.1 M, pH 7.0) containing 5 mM $K_3[Fe(CN)_6]/K_4[Fe(CN)_6]$. CV responses were recorded in potential of –0.2 to 0.6 V at scan rate of 100 mV s^{-1} and EIS was tested in potential of 220 mV (vs. SCE) with amplitude of 5 mV and frequency range of 1.0×10^{-2} Hz to 1.0×10^{6} Hz.

RESULTS AND DISCUSSION

TEM and UV-vis characterization of porous PtNTs:

TEM and UV-vis absorption spectra were used to verify the successful synthesis of TeNWs and porous PtNTs. From Figure S1, compared with TeNWs (Figure S1A), a number of PtNTs with a rough surface were observed (Figure S1C). TEM image of PtNTs at higher magnification (Figure S1D) clearly revealed the hollow nanostructure and holes in the shell of the nanotubes by comparison with that of TeNWs (Figure S1B). Additionally Figure S2 describes UV-vis absorption spectra of TeNWs and Te@Pt after re-dispersing in water for 3 h. Clearly, TeNWs showed two characteristic absorption peaks, while they almost disappeared at Te@Pt in water for 3 h. The results in good accordance with the reference[1] indicated TeNWs as sacrificial templates were disintegrated completely, leading to formation of porous PtNTs. The obtained results demonstrated the successful achievement of porous PtNTs.

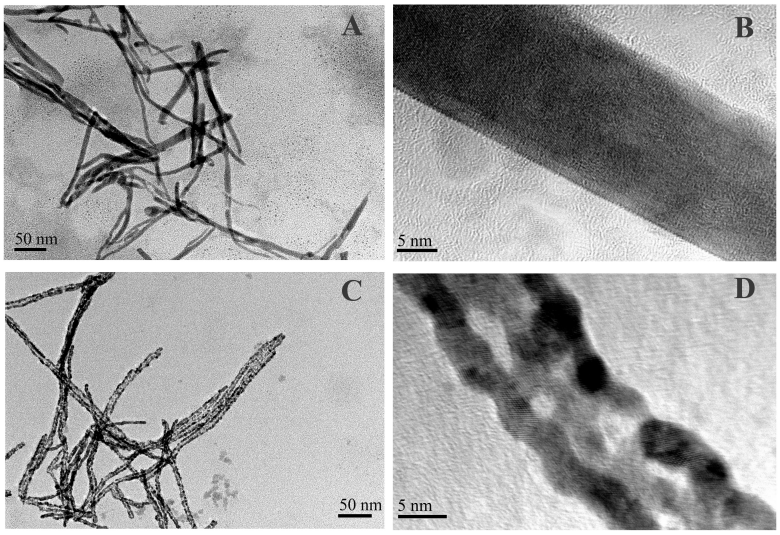

Figure S1 TEM images of as-synthesized TeNWs (A) and porous PtNTs (C). High-magnification TEM images of TeNWs (B) and porous PtNTs (D).

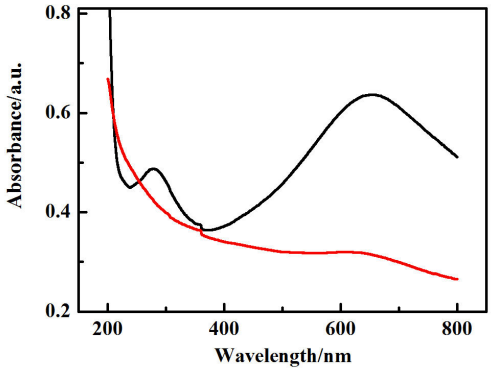

Figure S2 UV-vis absorption spectra of TeNWs (black line) and Te@Pt (red line) after re-suspending in water for 3 h.

Characterization of the proposed aptasensor:

CV and EIS which can indicate the change of surface area, resistance and carried charge could provide additional information about electrode surface modification. Thus, the assembly process of modified electrode could be monitored using CV and EIS techniques. Figure S3A represents the cyclic voltammograms (CVs) of different modified electrodes during the stepwise fabrication. The bare GCE exhibited an obvious redox peak (curve a). After electrodeposition of AuNPs, an increased peak current was obtained (curve b), as a result of the high conductivity of AuNPs for facilitation of electron transfer. When MPTS sol-HRP biocomposite was modified on the electrode, the peak current significantly decreased (curve c), which could be ascribed to the inert property of MPTS and enzyme. After that high conductive AuNPs was further loaded onto the electrode, the peak current dramatically increased (curve d) compared with that of MPTS sol-HRP/AuNPs/GCE. The first three modification steps of electrode were also observed by SEM images (Figure S4). Upon immobilization of TBA on the modified electrode, a decreased current was observed (curve e), indicating

that TBA hindered the tunnel of electron shuttle. Non-conductive HT as the blocking agent made the peak current decrease again (curve f). The incubation of TB (1 nM) led to further decrease of peak current (curve g), attributing to the formation of apatmer-TB complex on electrode surface which increased steric hindrance and blocked electron transfer. EIS results shown in Figure S3B were consistent with those obtained from CV measurements as mentioned above, which demonstrated the successful fabrication of aptasensor.

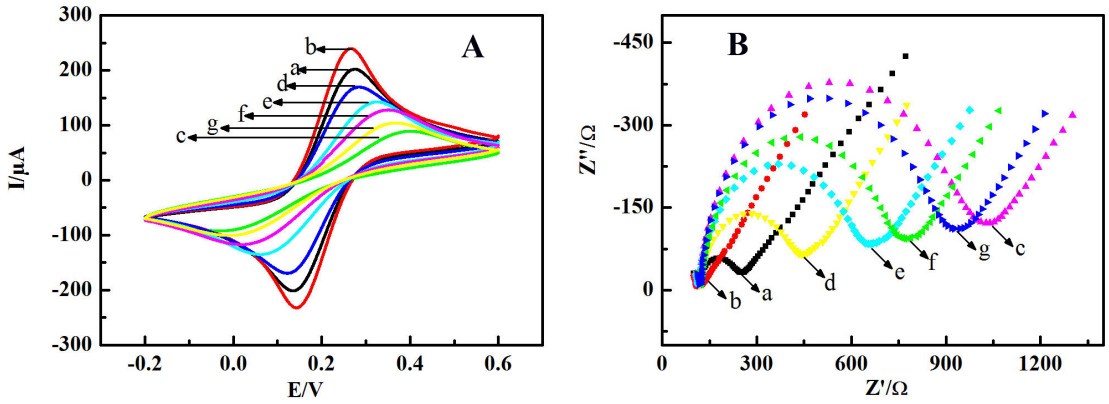

Figure S3 CV (A) and EIS (B) characterization of different modified electrode in 0.1 M PBS containing 5 mM $K_3[Fe(CN)_6]/K_4[Fe(CN)_6]$ (a) bare GCE, (b) AuNPs/GCE, (c) MPTS sol-HRP/AuNPs/GCE, (d) AuNPs/MPTS sol-HRP/AuNPs/GCE, (e) TBA/ AuNPs/MPTS sol-HRP/AuNPs/GCE, (f) HT/TBA/AuNPs/MPTS sol-HRP/AuNPs/ GCE, (g) TB/HT/TBA/AuNPs/MPTS sol-HRP/AuNPs/GCE. The scanning rate of CV is 100 mV S^{-1}. EIS was recorded in potential of 220 mV (vs. SCE) with amplitude of 5 mV and frequency range of 1.0×10^{-2} Hz-1.0×10^{6} Hz.

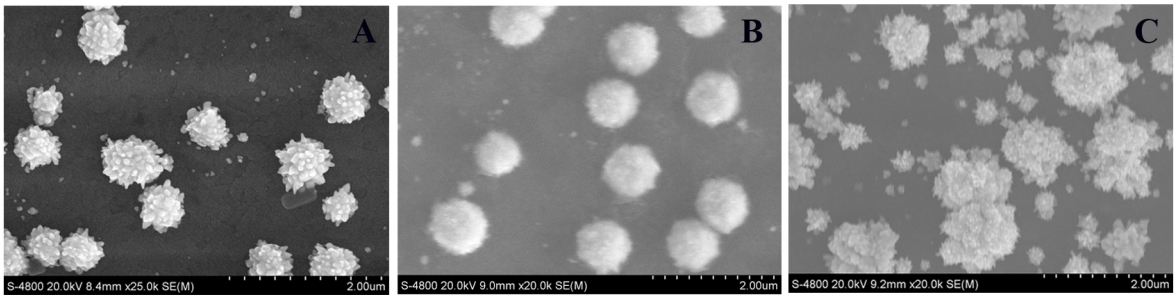

Figure S4 SEM images of AuNPs, MPTS sol-HRP/AuNPs, AuNPs/MPTS sol-HRP /AuNPs.

Selection of optimal experiment conditions:

Optimizing experiment conditions aims at improving the analytical performance of aptasensor and could further enhance electrochemical response for target TB. The influence of primary TBA concentration (0.5 μM, 1 μM, 1.5 μM, 2 μM and 3 μM) on the performance of aptasensor was firstly explored by CV in 0.1 M PBS (pH 7.0) containing 5 mM $K_3[Fe(CN)_6]/K_4[Fe(CN)_6]$. As shown in Figure S5A, the peak current was remarkably decreased with increment of primary TBA concentration and reached a plateau at 2 μM. So, the optimal concentration of primary TBA for the construction of aptasensor was 2 μM.

Highly efficient capture of TB is a key factor for a successful aptasensor. The incubation time for interaction between primary aptamer and TB was also studied. Figure S5B displays CV responses of the modified electrode for TB (1 nM) in 0.1 M PBS (pH 7.0) containing 5 mM $K_3[Fe(CN)_6]/K_4[Fe(CN)_6]$ under different incubation time (10 min, 20 min, 30 min, 40 min and 50 min). The results indicated peak current declined with the increase of time and tended to level off at 40 min, illustrating the saturation binding of aptamer-TB. Therefore, 40 min was adopted as the optimal

incubation time for TB detection.

In addition, optimizing the amount of H_2O_2 in testing buffer could enhance the bioelectrocatalytic efficiency and further improve the sensitivity of aptasensor. Figure S5C shows DPV responses of aptasensor for TB (1 nM) in 2 mL 0.1 M PBS (pH 7.0) in the presence of different concentrations of H_2O_2 (0.35 mM, 0.7 mM, 1.05 mM, 1.4 mM, 1.58 mM and 1.75 mM). As can be seen, DPV signal was gradually decreased with the increase of H_2O_2 concentration, and the peak current reached a stable value at 1.58 mM, predicting the highest efficiency of bioelectrocatalysis at this point. Thus, 1.58 mM of H_2O_2 was used in the following experiments.

The effect of pH of testing buffer on the electrochemical response of the proposed aptasensor was investigated by using DPV obtained in 0.1 M PBS (pH 5.0-9.0) with 1 nM TB and 1.58 mM H_2O_2, and the result is shown in Figure S5D. As could be seen, the best electrochemical signal of the proposed aptasensor was observed when tested in pH 7.0 PBS. So the subsequent investigation of the electrochemical performance was carried out in pH 7.0 PBS (0.1 M).

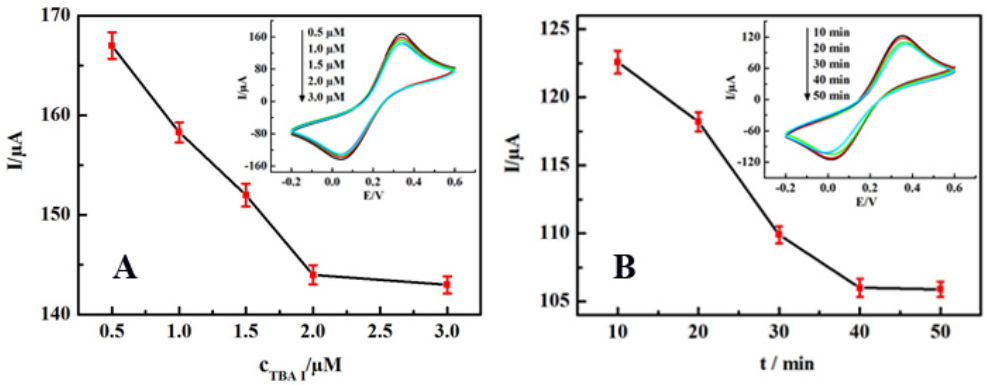

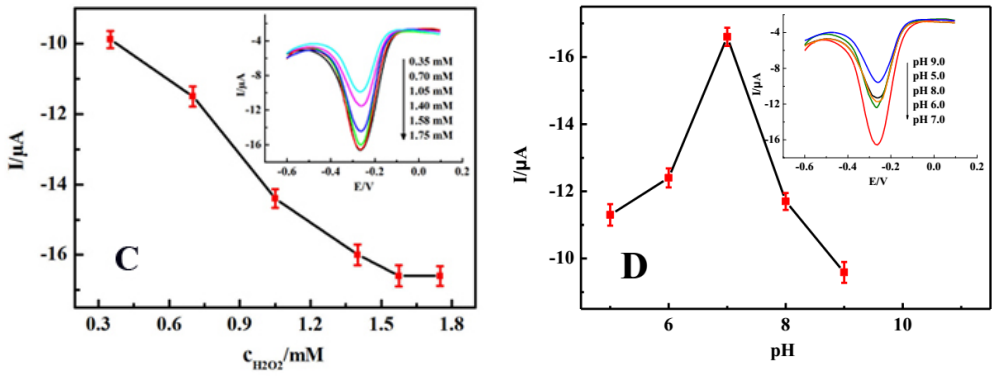

Figure S5 Effect of experiment conditions on the electrochemical response of the aptasensor: (A) concentration of primary TBA, (B) incubation time of target TB, (C) H_2O_2 concentration and (D) pH of testing solution buffer. CV or DPV responses are displayed in the inset. Measurements were carried out (A and B) at the scan rate of 100 mV s^{-1} in 5 mM $K_3[Fe(CN)_6]/K_4[Fe(CN)_6]$, and (C and D) in 0.1 M PBS (pH 7.0) with 1 nM TB and 1.58 mM H_2O_2. Error bars: SD, n=3.

Signal amplification performance of the proposed aptasensor:

In this strategy, PAMAM with dendritic nanostructure could increase the surface area of electrode and immobilize more redox-active Tb, resulting in the enhancement of electrochemical signal and improvement of sensitivity of aptasensor. To prove the effect of PAMAM on the electrochemical signal, two different secondary aptamer bioconjugates (PtNTs-PAMAM-Tb-TBA-BSA and PtNTs-Tb-TBA-BSA) were employed respectively. Figure S6A shows the DPV signals of different modified electrodes in 2 mL PBS (0.1 M, pH 7.0) buffer under optimal experimental conditions. For the modified electrode with PtNTs-PAMAM-Tb-TBA-BSA bioconjugate, a much stronger electrochemical signal was obtained (black line). In contrast, a poor electrochemical signal was observed at the modified electrode with

PtNTs-Tb-TBA-BSA bioconjugate (red line). Obviously, the employment of PAMAM enhanced the electrochemical signal, which paved the way for the fabrication of sensitive aptasensor. The amplified electrochemical signal was achieved by the corporate electrocatalysis of porous PtNTs and HRP toward H_2O_2 reduction. To verify the above view, DPV response of different modified electrodes (the inset in Figure S6B, C and D) for 1 nM TB were investigated in PBS buffer in the presence and absence 1.58 mM H_2O_2. The signal amplification efficiency (ΔI) of the aptasensor without PtNTs (Figure S6B) or without MPTS sol-HRP (Figure S6C) was lower than that of the proposed aptasensor (Figure S6D). The proposed aptasensor showed a more excellent bioelectrocatalytic activity toward H_2O_2 reduction and the efficiently amplified electrochemical signal as expected. These originated from the corporate bioelectrocatalysis of porous PtNTs and rich HRP in MPTS sol toward H_2O_2 reduction, and high loading of redox-active Tb based on dendritic PAMAM with numerous amine groups, which finally resulted in the excellent sensitivity of the proposed aptasensor in electrochemical detection.

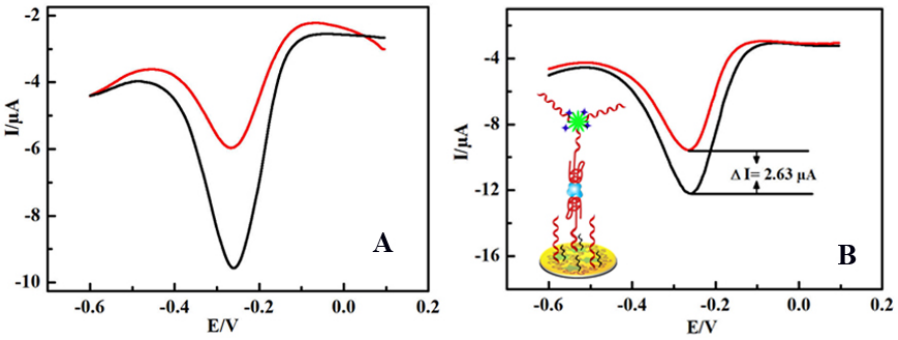

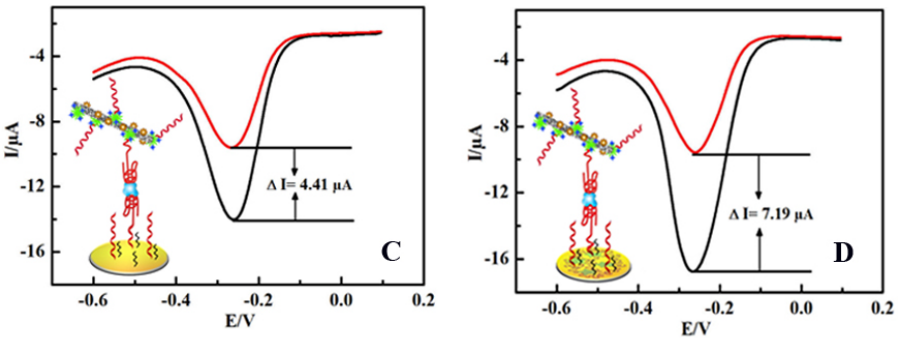

Figure S6 DPV responses of the aptasensor incubated with different bioconjugates: (A) PtNTs-PAMAM-Tb-TBA-BSA (black line) and PtNTs-Tb-TBA- BSA (red line) in 0.1 M PBS (pH 7.0). (B) Without PtNTs, (C) without MPTS sol-HRP and (D) with PtNTs-PAMAM-Tb-TBA-BSA in 0.1 M PBS (pH 7.0) with (black line) and without (red line) 1.58 mM H_2O_2.

The stability of the aptasensor:

After the aptasensor was incubated with 1 nM target TB, its CV response in 5 mM $K_3[Fe(CN)_6]/K_4[Fe(CN)_6]$ solution was investigated by 50 continuous cycle scans, and the result is shown in Figure S7. As can be seen, a 6.95% decrease of initial peak current was found, indicating the aptasensor had good stability.

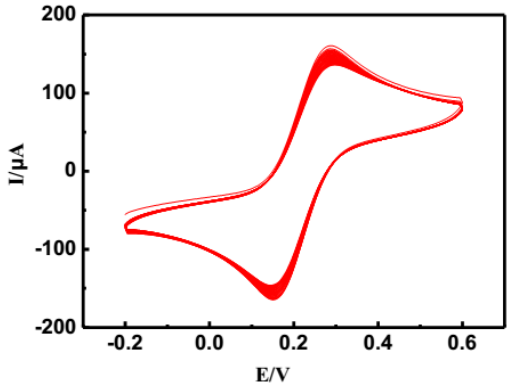

Figure S7 CV responses of the aptasensor incubated with 1 nM Target TB in 5 mM $K_3[Fe(CN)_6]/K_4[Fe(CN)_6]$ at the scan rate of 100 mV s^{-1}.

Table S1 Determination of thrombin added in human serum with the proposed aptasensor[a]

Samples	Added thrombin (nM)	Found thrombin (nM)[b]	Relative standard deviation (%)	Recovery (%)
1	0.001	0.000991	3.9	99.1
2	0.01	0.0106	5.0	106
3	0.1	0.103	4.4	103
4	10	9. 89	6.7	98.9
5	20	21.6	4.9	108

[a] The experimental measurements were accomplished by DPV in 0.1 M PBS (pH 7.0) containing 1.58 mM H_2O_2. [b] The values were the average of three measurements.

References

1 K. Cai, Z. H. Lv, K. Chen, L. Huang, J. Wang, F. Shao, Y. J. Wang and H. Han, *Chem. Commun.*, 2013, **49**, 6024.

2 Z. H. Lin, Z. Yang and H. T. Chang, *Cryst. Growth & Des.*, 2007, **8**, 351.

3 B. K. Jena and C. R. Raj, *Anal. Chem.*, 2006, **78**, 6332.